

A Study of Modelling and Inverter Controls for AC Microgrid Simulation

Cheng-Yu Yu, Gary W. Chang, *Member, IAENG*, Yu-Jen Liu, Raymond Y. Chang, and Yee-Der Lee

Abstract—In this paper the simulation of an AC microgrid integrated with distributed energy resources (DERs) to increase the renewable energy penetration and improve its operation reliability through different control strategies is presented. Under normal operation, the microgrid is connected to the utility grid through active/reactive power control for DERs and energy storage units. It also includes Voltage/Var control for the photovoltaic inverters to provide required reactive power. When the microgrid is disconnected from the utility grid due to external faults, the energy storage system will move to voltage/frequency control to maintain the microgrid voltage and frequency. Several scenarios including grid-connected and islanding modes with DER and energy storage unit controls are simulated. Results show that proposed control strategies for the microgrid perform as expected to maintain a stable operation of the microgrid.

Index Terms—Microgrid, photovoltaic, energy-storage system, voltage/var control

I. INTRODUCTION

Microgrids can manage and utilize the distributed energy resources (DERs) effectively. The advantages of distributed renewable generation include less emission of pollutants, high utilization of energy, less topographical restriction, and control flexibility. Microgrid concept assumes a cluster of loads and microsources operating as a single controllable system that provides both power and heat to its local area. Users can design the microgrid to meet their needs of electric power [1]. The microgrid can be regarded as a controlled cell of the power system. Many distributed energy resources are power electronic-based resources and controllable in the operation. These devices make energy sources more flexible. Energy storage systems are also used in the microgrid to enhance the reliability and supply the microgrid in islanding mode.

The microgrid is normally connected to the utility grid operated in grid-connected mode. In this mode, the microgrid control center (MGCC) commands every DER operated under active and reactive power (i.e. P/Q) control to provide the most economical output in accordance with the characteristics

Manuscript received March 2, 2017. This work was supported in part by Ministry of Science and Technology, Taiwan, under Grant MOST 106-3113-E-042A-001-CC2.

The authors are with the Department of Electrical Engineering, National Chung Cheng University, Min-Hsiung, Chia-Yi 621, Taiwan. (phone: +886-52729302; fax: +886-52720862; e-mail: garywkchang@gmail.com, azen0613@gmail.com, stu916466@gmail.com).

Raymond Y. Chang is with Institute of Nuclear Energy Research, Tao-Yuan, 32546, Taiwan. (e-mail: raymond@iner.gov.tw, ydlee@iner.gov.tw).

of the DER. When the microgrid is disconnected from the utility grid due to fault events, the MGCC will detect the islanding and command the specified DERs switch to Voltage/Frequency (i.e. V/F) control mode from P/Q control mode to maintain the power balance between the supply and load demand. The MGCC performs functions such as power monitoring, operations management, and load shedding mechanism [2]-[5].

In this paper, simulations of controlling the inverters of DERs and energy-storage units under different controls models to enable the AC microgrid to robustly work for both grid-connected and islanding modes are reported. An energy-storage battery in the microgrid adopts the P/Q control under the grid-connected mode and the P/Q control will switch to V/F control to maintain power balance under the islanding mode. The AC microgrid model under study is built by Matlab/Simulink and the proposed inverter control strategies are verified through results of Matlab/Simulink simulations. Results also show that the proposed control methods are efficient while the microgrid is under stable operation.

II. CONTROL METHODS OF DERs IN INER MICROGRID

A. Overview of INER Microgrid

The one-line diagram of the microgrid under study is depicted in Fig. 2, where microgrid of Institute of Nuclear Energy Research (INER) is the first autonomous hundred-kW 380-V microgrid in Taiwan with three-phase four-wire configuration and information, communication and control systems of the microgrid have been established. The static transfer switch (indicated by SS) is used to interconnect between three zones, Zone 1, Zone 2 and Zone 3, of the INER AC microgrid and the local electric utility. Zone 1 is in parallel with Zone 2 and Zone 2 is in series connection with Zone 3. The *rms* line voltage of distribution grid is 380 V and the frequency is $f_s=60$ Hz.

Distributed energy resources in the microgrid are photovoltaics, wind turbines, and microturbines. The energy storage system (ESS) can be used to regulate power flow and power factor under grid-connected operation and stabilize the system during the islanding operation or changing the operation mode. The controllable load banks in Zone 1 and Zone 2 consist of single-phase and three-phase loads. There is the only one single-phase load bank in Zone 3.

B. Three-Phase Active and Reactive Control

The P/Q control is proposed to control each DER inverter to output a preset or maximum power according to the DER characteristics. In this mode the *abc* to *dq0* reference frame

transformation is adopted to calculate the reference real and reactive power output of the inverter, where the transformation matrices are given in (1) [6].

To help maintain the microgrid operated at the nominal voltage and frequency, the DER inverters in the microgrid are controlled by three different methods when connecting to the utility grid, as shown in Fig. 2. In Fig. 2, the voltage source inverter (VSI) of a DER is controlled by the PI controller to determine the inverter output voltage and current and thus maintain the voltage and frequency at the point of common coupling (PCC) [7].

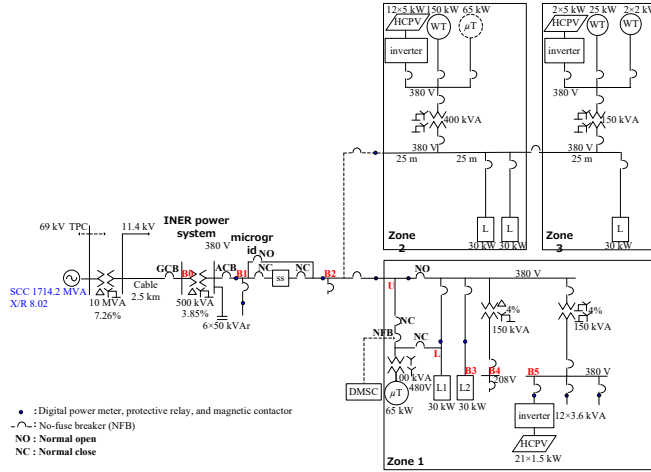


Fig. 1. Structure of the INER microgrid including three zones.

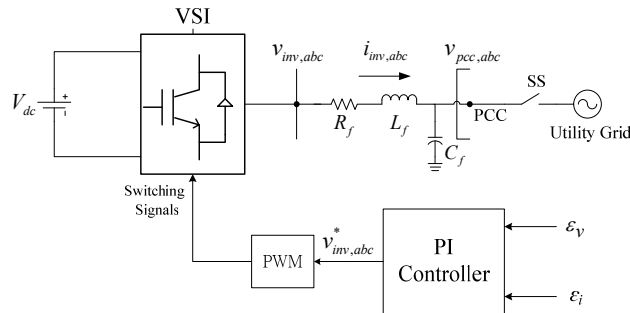


Fig. 2. Control mechanism of the microgrid DER.

$$\begin{pmatrix} v_d \\ v_q \\ v_0 \end{pmatrix} = [C] \cdot \begin{pmatrix} v_a \\ v_b \\ v_c \end{pmatrix}, \quad \begin{pmatrix} i_d \\ i_q \\ i_0 \end{pmatrix} = [C] \cdot \begin{pmatrix} i_a \\ i_b \\ i_c \end{pmatrix} \quad (1)$$

$$\text{where } [C] = \frac{2}{3} \begin{bmatrix} \cos(\omega t) & \cos(\omega t - \frac{2\pi}{3}) & \cos(\omega t + \frac{2\pi}{3}) \\ \sin(\omega t) & \sin(\omega t - \frac{2\pi}{3}) & \sin(\omega t + \frac{2\pi}{3}) \\ \frac{1}{\sqrt{2}} & \frac{1}{\sqrt{2}} & \frac{1}{\sqrt{2}} \end{bmatrix},$$

and $w = 2\pi f_s$.

The P/Q control is mainly achieved by controlling the real and reactive reference currents in d - and q -axis. Equation (2) shows the power calculation in the $dq0$ reference frame. Since v_q is 0, the inverter output reference current is given by (3).

$$\begin{cases} P_{ref} = 2(v_d i_d + v_q i_q) / 3 \\ Q_{ref} = 2(v_q i_d - v_d i_q) / 3 \end{cases} \quad (2)$$

$$\begin{cases} i_{dref} = \frac{2 P_{ref}}{3 v_d} \\ i_{qref} = -\frac{2 Q_{ref}}{3 v_d} \end{cases} \quad (3)$$

As illustrated in Fig. 2, after determining the reference current signals of (3), they are compared with the real inverter output currents and then obtain the error signals, ϵ_i and ϵ_v . The error signals are applied to the PI controllers, and their outputs are computed with $v_{pcc,d}$, $v_{pcc,q}$, $i_{inv,d}wL$ and $i_{inv,q}wL$ terms to generate the reference voltages, $v_{inv,d}^*$ and $v_{inv,q}^*$ [8-10]. Then, the switching signals are produced by PWM and are input to the VSI. Figure 3 depicts the control block diagram to determine inverter reference output voltages in $dq0$ reference frame. The abc reference voltages are then obtained by (1).

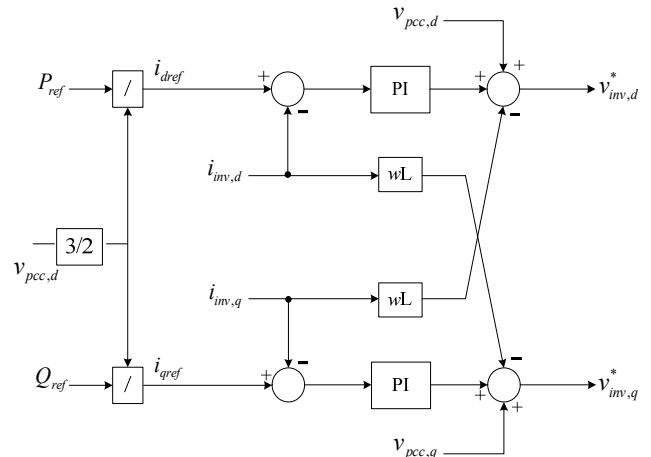


Fig. 3. Control block diagram for determining inverter reference output voltages.

C. Three-Phase Volt/Var Control

The Volt/Var control is implemented to supply the reactive power output based on controlling the PV inverter voltage magnitude [11]. In the Volt/Var control, the voltage control is accomplished with a linear droop characteristic, which determines the reactive power injection as a function of the voltage magnitude at the PV inverter terminals [12]. Figure 4 shows the functional blocks of the three-phase Volt/Var controller and the inverter Volt/Var droop characteristic.

The Volt/Var control is to obtain the active power output of PV to compute maximum reactive power of (4), which is to limit the output without exceeding the inverter apparent power rating, S , and then determine the microgrid voltage magnitude for the droop function to compute the reactive power output. If the reactive power output is within the limit, the PV output is to maintain voltage magnitude that meets the regulation requirement.

$$Q_{max} = \sqrt{S^2 - P^2} \quad (54)$$

The control is recomputed at every fundamental period based on the active power and the apparent power rating of the inverter. In Fig. 4(a) $Q(-)$ is zero within the deadband since the voltage is within the preset voltage range (e.g. between 0.97 pu and 1.03 pu). When the measured voltage exceeds V_b shown in Fig. 4(b), the inverter starts absorbing reactive power and reduces the voltage gradually. At V_b and above, the inverter is asked to absorb the maximum reactive

power within the limit. This is a commonly seen PV operating mode because of the voltage rise phenomenon caused by PV system. Nevertheless, this controller can also contribute to the mitigation of low-voltage situation such as the locations are remote from the substation under heavy load conditions, when the voltage drops below V_a shown in Fig. 4(b).

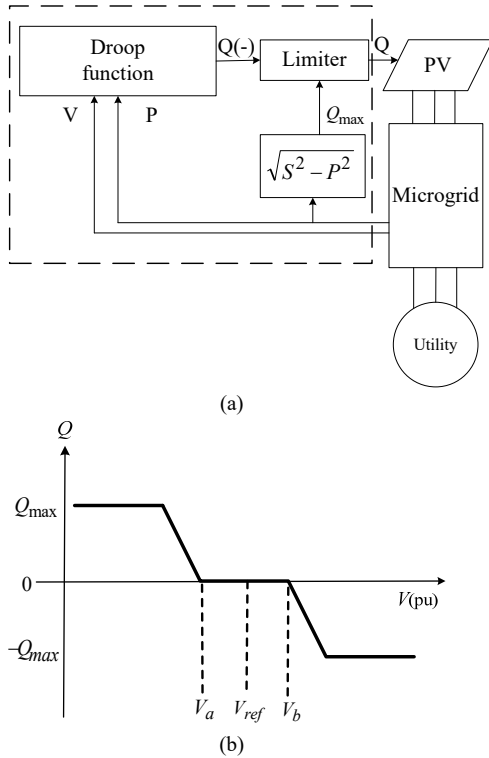


Fig. 4. (a) Block diagram of a PV inverter with Volt/Var controller, (b) the droop function.

D. Volt/Var Control of Single-Phase Inverter

The Volt/Var control is also used in the single-phase inverter. For such inverters, a widely-used control scheme is to model three-phase inverter through time delay, which is to convert the 3-phase AC system to a 2-phase system using the Park transformation and then convert to a 2-phase dc system [13]. Another control method is to use a different algorithm to control the inverter. In the proposed control scheme, the active power (P) and reactive power (Q) of the single-phase inverter are shown in (5), respectively.

$$\begin{aligned}
 P &= \frac{V_c V_t}{X_l} \sin \alpha \approx \frac{V_c V_t}{X_l} \alpha \\
 Q &= \frac{V_t}{X_l} (V_c \cos \alpha - V_t) \approx \frac{V_t}{X_l} (V_c - V_t)
 \end{aligned}
 \tag{5}$$

where V_c and V_t are the inverter *rms* output voltage V_c and the PCC voltage V_t , α is the phase angle difference of V_c and V_t , and X_l is the equivalent reactance of the transformer.

Thus, the active power is controlled by regulating the phase angle difference α of V_c and the reactive power is controlled by the regulating of the V_c and V_t . The simulation model is shown in Fig. 5, where the proposed decoupled control algorithm can control the inverter's active power and reactive power independently and instantaneously. The fast response of the control algorithm ensures that the PV system can provide service under different system conditions, both in steady and transient states and in grid-connecting and islanding modes.

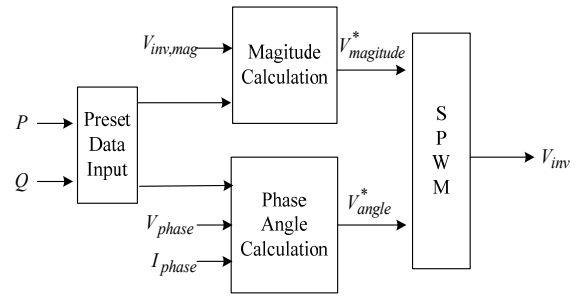


Fig. 5. Single-phase inverter Volt/Var control.

E. Voltage/Frequency Control

If a cluster of DERs is operated within a microgrid connected to the utility network, all the inverters can be operated in P/Q mode because the microgrid has the voltage and frequency references. However, to operate the microgrid in islanding mode a voltage source inverter can be used to provide a reference for frequency and to smoothly switch to islanding operation without changing the control mode of any other inverters.

The inverter output frequency is a produced sine wave signal inside the controller. That signal is used as a directional reference vector, which is in the d -axis of the $dq0$ reference frame. In this reference frame, the value of d -axis and q -axis output voltages are

$$V_{dref} = U_0, \quad V_{qref} = 0 \tag{6}$$

where both V_{dref} and V_{qref} are the reference of the d -axis and q -axis *rms* voltages, respectively. When the microgrid operates at nominal voltage, $U_0 = 1$ pu.

To achieve the voltage control, it usually uses voltage and current double close-loop controls. Voltage loop adjusts the magnitude of the output voltage. The output of voltage loop serves as the current loop input reference. The output current references of the voltage loop are given in (7).

$$\begin{cases}
 i_{dref} = \left(K_{pdu} + \frac{K_{idu}}{s} \right) (V_{dref} - V_d) \\
 i_{qref} = \left(K_{pdu} + \frac{K_{iqu}}{s} \right) (V_{qref} - V_q)
 \end{cases}
 \tag{7}$$

The output voltages of the current loop are given in (8).

$$\begin{cases}
 V_{id} = V_d + wL i_q + \left(K_{pd} + \frac{K_{id}}{s} \right) (i_{dref} - i_d) \\
 V_{iq} = -wL i_d + \left(K_{pq} + \frac{K_{iq}}{s} \right) (i_{qref} - i_q)
 \end{cases}
 \tag{8}$$

Figures 6 and 7 depict the functional blocks of the double control loops.

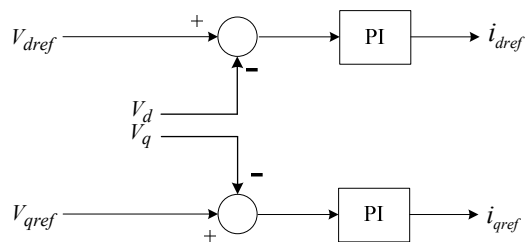


Fig. 6. Control block diagram of voltage loop.

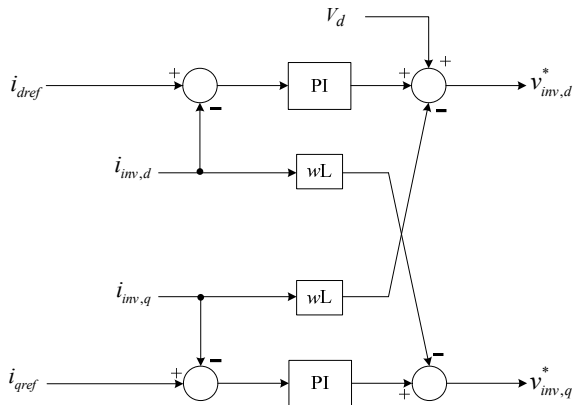


Fig. 7. Control block diagram of the current loop.

When the fault occurs at the utility grid side, the microgrid will be disconnected from the grid. MGCC will detect the current drop at PCC and commands the energy storage system to operate at V/F control mode. When the fault is clear, MGCC will decide when the microgrid is reconnected to the grid based on the synchronization conditions related to phase sequence, frequency, and voltage deviations.

III. REVIEW OF THREE INVERTER CONTROL STRATEGIES

Microgrid has many different control strategies for different operation scenarios. In this paper, P/Q control, droop control, and V/F control of inverters are used in grid-connecting and islanding modes. P/Q control is adopted in all DERs except the DER is under islanding control. The P/Q control can generate the preset power (P_{ref} and Q_{ref}) to the grid and is independent of microgrid voltage and frequency, as shown in Fig. 8.

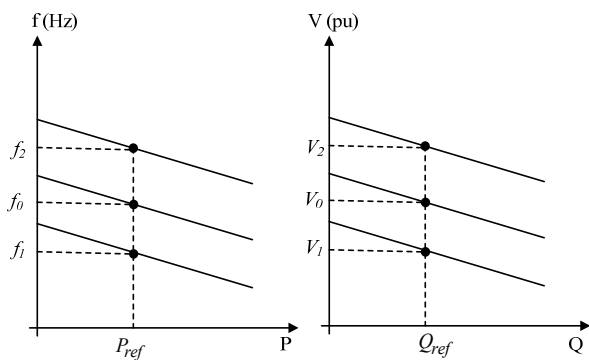


Fig. 8. Frequency and voltage droop characteristics under P/Q control.

Droop control will change the output power which is varied with the microgrid voltage and frequency [14]. If the microgrid voltage and frequency are dropped, the DERs/energy storage systems will increase the active and reactive power output. Droop control can be used in two or more DERs which are controllable to supply power to the microgrid, as shown in Fig. 9.

V/F control will change the power output of the energy storage system to maintain the microgrid voltage and frequency at nominal values. Figure 10 illustrates the V/F control characteristics of an inverter.

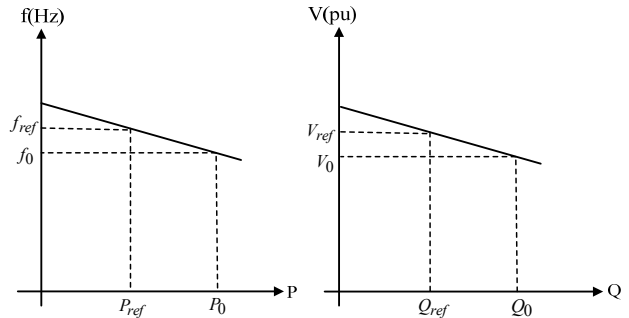


Fig. 9. Droop control for frequency and voltage.

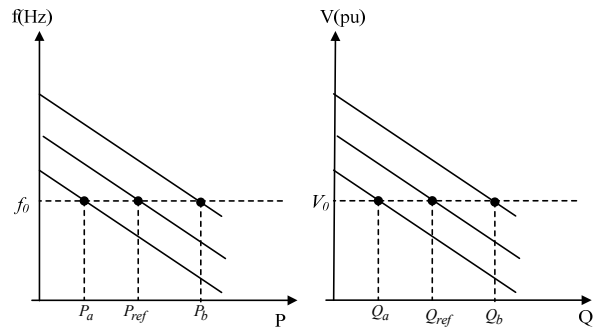


Fig. 10. Frequency and voltage droop characteristics under V/F control.

IV. CASE STUDY

This paper applies Matlab/Simulink to develop the 380-V and 60-Hz INER three-zone microgrid model, as shown in Fig. 1. To simplify the modelling task and focus on assessing the effectiveness of the inverter controls of DERs and energy storage systems, most DERs are modeled as constant dc-voltage sources. The Simulink model of Fig. 1 is depicted in Fig. 11. The structure of the Zone 1 is illustrated in Fig. 12. There are three DERs and two controllable loads in Zone 1. Zone 2 includes a wind turbine and PV systems and Zone 3 includes a wind turbine and a microturbine. The microgrid is connected to the utility grid by a static transfer system (SS). Due to the space limit, only simulation parameters for Zone 1 are listed in Table 1.

The purpose of the study case is to simulate the INER microgrid operated in grid-connected and islanding modes. The initial total generation and load conditions at each zone for the simulation are given in Table 2, where the DERs and loads are dispatchable and controllable. The simulation scenarios are indicated in Table 3. At first, all three zones are operated at the predetermined output power settings under the P/Q mode. At 0.6 s, the microgrid switches to islanding mode due to a fault occurred at the utility grid side. To meet the load demand, the energy storage system in the Zone 1 is switched to V/F control mode and regulates the power output to maintain the microgrid voltage and frequency. At 1.4 s, the microturbine in Zone 1 increases its output power to 0.2 pu to take over the decreasing power output of the energy storage system. At 1.6 s, the MGCC detects the fault is cleared, and checks the differences of the voltage, frequency and phase between the microgrid and the utility grid [15]. The frequency and the rms voltage of the microgrid during the simulation are shown in Fig. 13. The voltage and current waveforms in three zones are also shown in Fig. 14. By observing simulation results, the microgrid is well performed and operated stably.

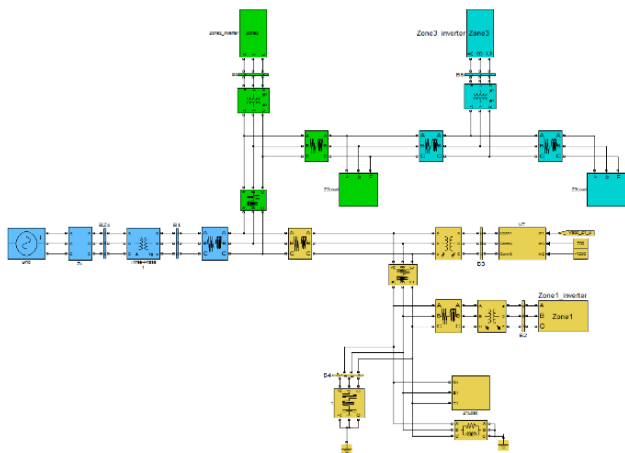


Fig. 11. Simulink model of the INER microgrid.

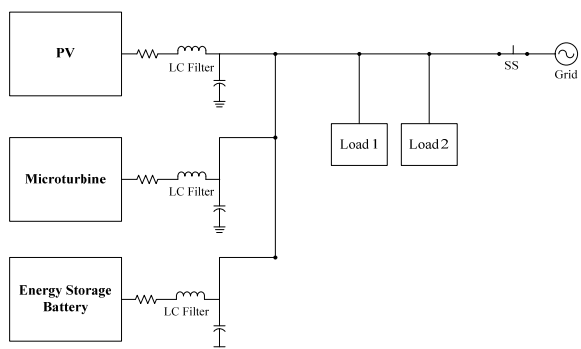


Fig. 12. Structure of Zone 1 of the microgrid.

Table 1. Simulation parameters for Zone 1

Parameters		Values
Energy Storage System	Inverter switching frequency	10 kHz
	Inverter filter inductance	2 mH
	Inverter filter capacitance	68.5 μ F
	DC-link voltage	700 V
	Maximum active power	60 kW
	Maximum reactive power	100 kVAr
PV system	Inverter switching frequency	10 kHz
	Inverter filter inductance	2 mH
	Inverter filter capacitance	68.5 μ F
	DC-link voltage	700 V
	Maximum active power	51.5 kW
Microturbine	Inverter switching frequency	10 kHz
	Inverter filter inductance	2 mH
	Inverter filter capacitance	68.5 μ F
	DC-link Voltage	700 V
	Maximum active power	31.5 kW
PI Controller	K_p P/Q	5
	K_i P/Q	500
	K_p V/F	6
	K_i V/F	30

TABLE 2. THE INITIAL CONDITIONS IN ZONE 1 TO ZONE 3 SYSTEMS

	Initial condition
Zone 1	40 kW (0.4 pu)
Load 1	30 kW (0.3 pu)
Zone 2	40 kW (0.4 pu)
Load 2	60 kW (0.6 pu)
Zone 3	40 kW (0.4 pu)
Load 3	30 kW (0.3 pu)

TABLE 3. SIMULATION SCENARIOS OF THE THREE-ZONE MICROGRID

Event	Operation condition	Time (s)
0	Three zones operated normally	0
2	A fault occurred at the utility grid side Microgrid operated under islanding mode	0.6
3	Microturbine started output 0.2 pu active power	1.4
4	Microgrid back to grid-connected mode	1.6

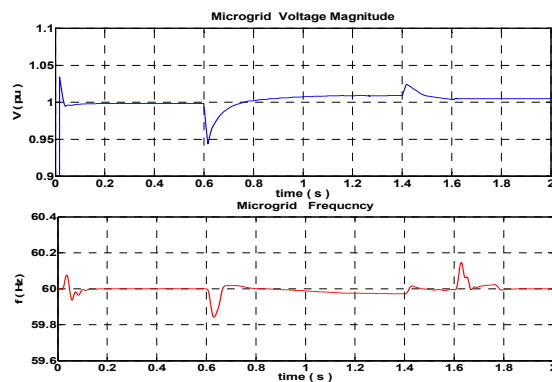


Fig. 13. RMS voltage and frequency of the microgrid.

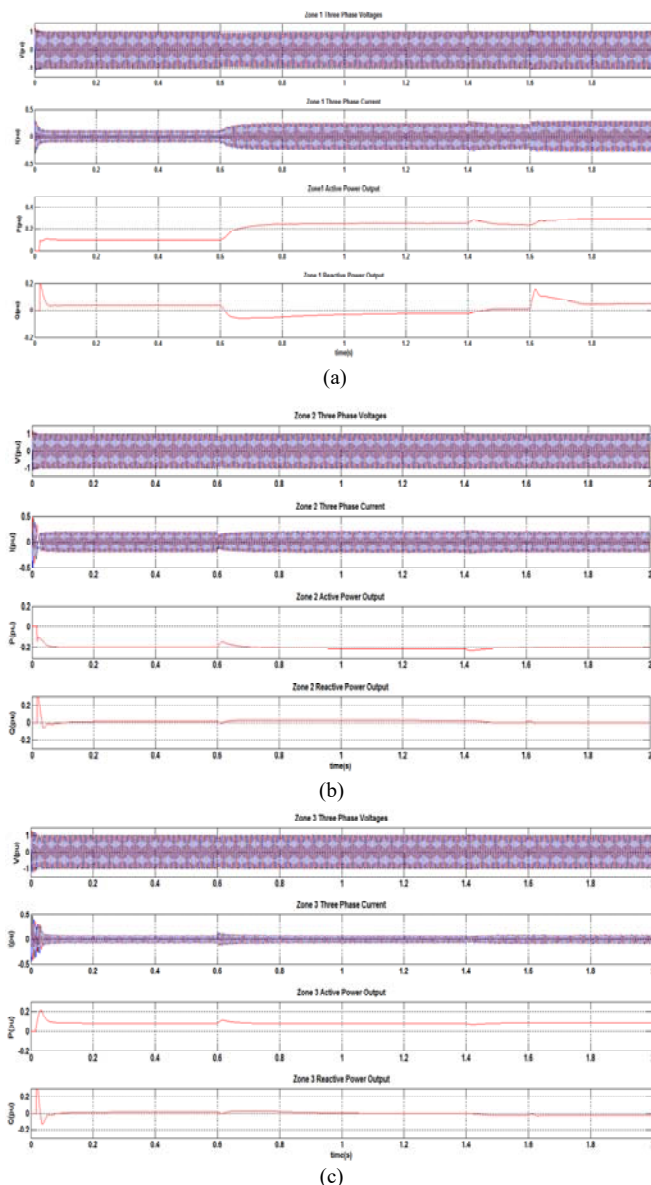


Fig. 14. Three-phase voltages, three-phase currents, active and reactive power output of (a) Zone 1, (b) Zone 2, and (c) Zone 3 for the study case.

V. CONCLUSION

In this paper, the inverter controls that adopted for DERs and energy-storage system in the microgrid have been presented. The inverter control is implemented to deal with the microgrid for normal operation under both grid-connected and islanding modes. Under the grid-connected mode, the DERs generate the predetermined power according to the characteristics of the DER units. The PV Volt/Var control is used to control the voltage magnitude of the microgrid. The single-phase PV system is also included in the system. When the islanding is detected, the microgrid is disconnected from the utility grid, which is commanded by the MGCC. At the same time, the energy storage system switches to V/F mode from P/Q mode to provide active power to critical loads and maintain the voltage and frequency of the microgrid.

The performances of the described inverter controls are verified through simulations using Matlab/Simulink. Results show that the functions of the controllers adopted in the study performs as expected. The microgrid can reliably operate either under grid-connected or islanding mode.

REFERENCES

- [1] N. Jayawarna, X. Wu, Y. Zhang, N. Jenkins, and M. Barnes, "Stability of a MicroGrid," *Proc. 3rd IET International Conference on Power Electronics, Machines and Drives*, pp. 316-320, March 2006.
- [2] J. A. P. Lopes, C. L. Moriera, and F. O. Resende, "Control strategies for microgrids black start and islanded operation," *Int. J. Distrib. Energy Res.*, vol. 1, no. 3, pp. 241-261, 2005.
- [3] B. S. Hartono, Y. Budiayanto, R. Setiabudy, "Review of microgrid technology," *Proc. International Conference on QiR (Quality in Research)*, pp. 127-132, June 2013.
- [4] M. Milosevic and G. Andersson, "Generation control in small isolated power systems," *Proc. 37th North Amer. Power Symp.*, pp. 524-529, 2005.
- [5] R. H. Lasseter et. al., "Integration of Distributed Energy Resources: The CERTS MicroGrid Concept," Lawrence Berkeley National Laboratory, *LBNL-50829*, April 2002.
- [6] M. G. Villalva, J. R. Gazoli, and E. R. Filho, "Comprehensive Approach to Modeling and Simulation of Photovoltaic Arrays," *IEEE Trans. on Power Electronics*, Vol. 24, No. 5, May 2009.
- [7] P. Piagi and R. H. Lasseter, "Autonomous control of microgrids," *Proc. 2009 IEEE PES General Meeting*, Montreal, July 2006.
- [8] C. Jin, P. C. Loh, P. Wang, Y. Mi, and F. Blaabjerg, "Autonomous operation of hybrid ac-dc microgrids," *Proc. 2010 IEEE Int. Conf. Sustainable Energy Technologies (ICSET)*, Sri Lanka, 2010.
- [9] M. Saeedifard, M. Graovac, R. F. Dias, and R. Iravani, "DC power systems: Challenges and opportunities," *Proc. 2010 IEEE PES General Meeting*, July 2010.
- [10] S. R. Guda, C. Wang, and M. H. Nehrir, "A Simulink-based microturbine model for distributed generation studies," *Proc. 37th Annu. North Amer. Power Symp.*, pp. 269-274, 2005.
- [11] P. Jahangiri and D. C. Aliprantis, "Distributed volt/var control by PV inverters," *IEEE Trans. Power Syst.*, vol. 28, no. 3, pp. 3429-3439, Aug. 2013.
- [12] Y. Xu, H. Li, D. T. Rizy, F. Li, and J. D. Kueck, "Instantaneous active and nonactive power control of distributed energy resources with a current limiter," *Proc. 2010 IEEE Energy Conversion Congr. Expo*, pp. 3855-3861, 2010.
- [13] V. Dixit, M. B. Patil, M. C. Chandorkar, "Real Time Simulation of Power Electronic Systems on Multi-core Processors," *Proc. 2009 International Conference on Power Electronics and Drive Systems*, pp. 1524-1529, Nov. 2009.
- [14] G. W. Chang, G. F. Zeng, H. j. Su, and L. Y. Hsu. "Modelling and simulation for INER AC microgrid control," *Proc. 2014 IEEE PES General Meeting*, July 2014.
- [15] *IEEE Standard for Interconnecting Distributed Resources to Electric Power Systems*, IEEE Standard 1547-2003.